

NUMERICAL INVESTIGATION EFFECT OF SHALLOW WATER ON SHIP RESISTANCE USING RANS METHOD

Tran Ngoc Tu¹

¹Vietnam Maritime University, Faculty of Ship building
tutn.dt@vimaru.edu.vn

Abstract: On inland waterways the ship resistance and propulsive characteristics are strictly related to the depth of the waterway, thus it is important to have an understanding of the influence of shallow water on ship motions to make inland vessels more economically competitive and reduce their fuel consumption, therefore accurate predictions of hydrodynamic forces in restricted waterway are required and important. This paper is aimed to predict ship resistance in shallow water by using commercial unsteady Reynolds–Averaged Navier – Stokes (RANS) solver. Volume of fluid (VOF) was applied for simulation of free surface flow around the ship. A comparison in the resistance on the hull is illustrated between shallow water and deep water. The numerical results obtained were validated against related experimental studies available in the literature.

Keywords: ship resistance, shallow water, RANS

Classification numbers: 2.1

1. Introduction

The behaviour of an inland vessel in restricted waterways is fundamentally different from that of a seagoing ship in open waters. When a ship navigates in shallow water, a number of changes occur due to the interaction between the ship and the seabed. There is an effective increase in velocity, backflow, decrease in pressure under the hull and significant changes in dynamic trim and sinkage. This leads to increases in potential and skin friction resistance, together with an increase in wave resistance and change propulsive characteristics.

Influence of water depth on resistance to predict hydrodynamic forces in confined waters to make inland vessels more economically competitive and reduce their fuel consumption.

Recently, there are three methods are used to evaluate ship resistance in shallow water, such as using empirical methods; using Computational Fluid Dynamics (CFD) method; performing model tests in towing tank.

The model tests give the most reliable result in comparison with two other above-mentioned methods for predicting ship resistance, but this technique is both expensive and time consuming, so this method is only used after the stage of alternative design, at which dimensions as

well as lines plan of ship have been already optimally chosen.

Using empirical methods based on towing tank results, such as method proposed by Artjushkov [1], Geerts [2], Karpov [3] to predict ship resistance in shallow water. The advantages of this method are fast and do not require much input data. However their range of application often fall out for inland ships and the lack of accuracy are a problem [4].

Nowaday, the fast development of computation resources is making Computation Fluid Dynamic (CFD) becoming a powerful tool for ship designers in solving the problems related to. Ship resistance calculation is one of the basic hydrodynamics problems. The benefits of this method is that they allow the visualization of several quantities - such as the flow streamlines, the wave profiles or the pressure distribution - that are difficult to obtain from experiments. This is a very useful aid for designers to understand the physics of the flow phenomena, at least from a qualitative point of view.

Depending on the assumption to simplify the fluid equations, there are some CFD approaches are available to solve hydrodynamics problems such as: potential flow theory (panel code), Reynold Averaged Navier-Stokes Equations (RANSE) and Large Eddy Simulation (LES). LES makes extensive

use of computer power rather than solving a large number of modeled equations as is the case for RANS models [5]. Thus, at the moment, the most popular approach is RANSE CFD, due to sufficient accuracy for engineering purposes at reasonable computational time. However, level of accuracy of the numerical simulation significantly depends on human skills. Thus this paper presents the theoretical background and application of the RANS method to investigate effect of shallow water on ship resistance. The case study is US Navy Combatant DTMB with available experiment data. So the result is validated with experiment. The commercial solver Star-CCM+ is used in this study.

2. Shallow water effects on ship wave patterns and ship resistance

Classification of water as deep or shallow is based on the ratio of water depth h to wavelength λ , where h is the water depth and λ is the wave length.

For the deep water the ratio h/λ is suitable for approximately $h/\lambda \geq 1/2$.

For the shallow water the ratio h/λ is suitable for approximately $h/\lambda \leq 1/20$ and $c = \sqrt{gh}$ is known as the critical speed, where c is wave velocity and g is the acceleration gravity.

Havelock [6] performed shallow water investigations in which he showed the wave patterns being formed due to a point source in shallow water. His work led to the introduction of the non-dimensional depth Froude number:

$$Fr_h = \frac{V}{\sqrt{gh}} \quad (1)$$

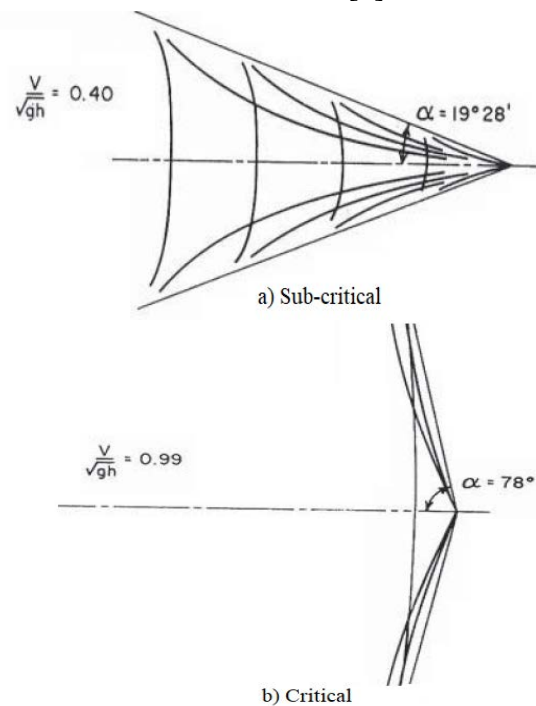
2.1. Shallow water effects on ship wave patterns

Evidently, the geometry of a ship's wave pattern in shallow water not only depends on its Froude number but also on its depth Froude number, which modifies the wave lengths and thus the interference of wave components.

Based on the value of Fr_h there are three flow regimes:

- Sub-critical $Fr_h < 1.0$;
- Critical $Fr_h = 1.0$;
- Supercritical $Fr_h > 1.0$.

At speeds well below $Fr_h < 1.0$, the wave system is as shown in Figure 1(a), with a transverse wave system and a divergent wave system propagating away from the ship see like the Kelvin wave pattern. When ship speed come to the critical speed, $Fr_h = 1.0$, the waves approaches perpendicular to the track of the ship, figure 1(b). At speeds greater than the critical speed, the diverging wave system returns to a wave propagation to the path of the ship with some angle, but in this case transverse waves are visible [6].



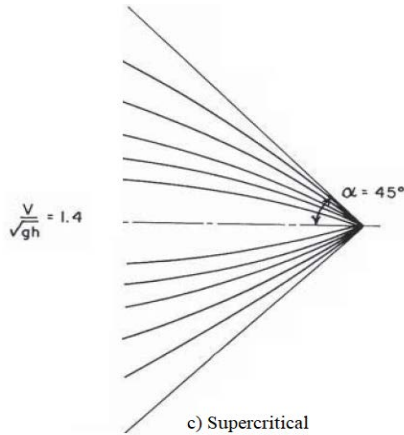


Fig.1 Change of wave pattern of a pressure patch with varying Fr_h according to [6].

2.2. Shallow water effects on ship resistance

In order to describe fully the effects of shallow water, it is usually to use a parameter such as T/h or L/h as well as depth Froude number Fr_h . The influence of shallow water on the wave resistance component caused by these changes in wave pattern has already been investigated by Havelock [6]. The results of resistance experiments based on Froude number regarding to the changes in L/h are shown in figure 2.

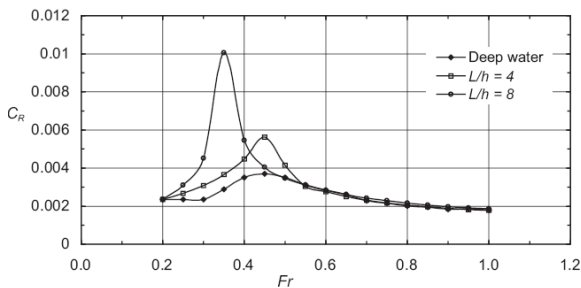


Fig.2. Influence of water depth on residual resistance coefficient [7].

Figure 3 shows the influence of water depth on total resistance coefficient base of Froude number regarding to the changes the depth Froude number.

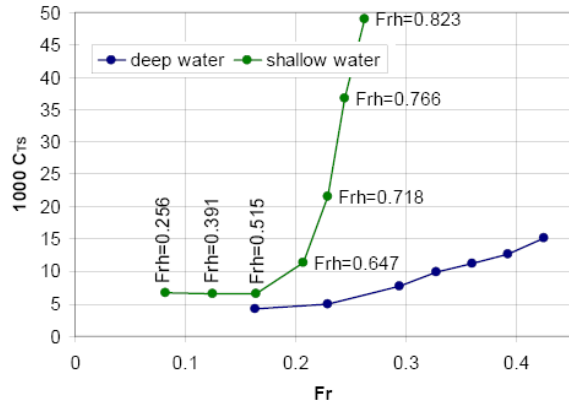


Fig.3 Influence of water depth on total resistance coefficient.

3. Numerical simulations

3.1. Reference vessel

The vessel under study in this paper is a US Navy Combatant DTMB shown in Figure 4. The main reason for using this hull is that extensive model test data exists for resistance at different Froude numbers in shallow water and in deep water [8,9]. The principal dimension of the DTMB are listed in the table 1, the tests conditions were carried out at model scale $\lambda = 26.69$ from the Ship Design and Research Centre CTO S.A, Poland.



Fig. 4. Geometry of US Navy Combatant DTMB.

Tab.2 Main particulars of the DTMB.

Description	Ship	Model
Scale factor	λ	-
Length between perpendiculars	$L_{pp}(m)$	142.0
Length of waterline	$L_{WL}(m)$	142.0
Breadth	$B(m)$	18.9
Draft	$T(m)$	6.16
Volume	$\nabla(m^3)$	8425
Wetted surface	$S(m^2)$	2949
Longitudinal Center of Buoyancy From AP	LCB/ L_{pp}	4.14
		0.489

3.2. Test cases

Computations were performed for the following conditions: design draft $T = 0.23$ m with volume of the model $\nabla = 0.455$ m³ and LCB measured from AP equal to 2.602m, the water deep $h = 0.4$ m.

The following parameters were considered in the simulations:

- Five depth Froude number: 0.302, 0.502, 0.604, 0.703, 0.755 corresponding to five ship speeds 0.598; 0.995; 1.196; 1.394; 1.495 m/s.
- The vessel is free to trim and sink;
- The hull mass is constant.

3.3. Computation setup

The commercial package Star-CCM+ from Siemens was used for the computation.

3.3.1. Computational domain and boundary conditions

Due to flow symmetry hence in order to reduce computational time, only the half of the hull (port side) is simulated.

Based on the recommendations and applications reported in Star-CCM+ [10], to avoid any wave reflection from the boundary walls, the size of computational domain chosen for used in this work as follow: inlet boundary is located at $1.5L_{PP}$ from forward perpendicular, while outlet boundary is located at $2.5L_{PP}$ from aft perpendicular. Top boundary is located at $1.0L_{PP}$ from the free surface. Lateral boundary is located at $1.5L_{PP}$ from the centre plane. For the bottom boundary is located at 0.4m (depth of water in this study) from the free surface. The free surface is located at $z=0$.

For boundary conditions, the following boundary conditions were applied for simulation ship resistance in shallow water:

- Velocity inlet was used on inlet and top tanks;
- No-slip wall condition on the hull;
- Moving No-slip wall (The bottom moves with a velocity equal to speed of ship) was applied on tank bottom;
- At outflow, the hydrostatic pressure was specified.

Symmetry condition (i.e. zero-gradient in normal direction) at symmetry plane and side tank.

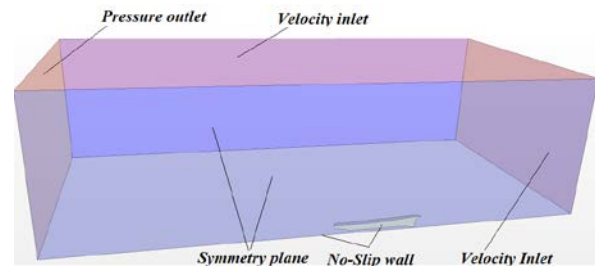


Fig. 5 General view of computational domain and applied boundary conditions.

3.3.2. Physics modelling

The computation was carried out using unsteady Reynold Averaged Navier-Stokes equations (RANS) model. The free surface was modelled with the volume of fluid (VOF) method. To simulate the turbulence in the fluid, the Realizable K-epsilon Two-layer was employed with the Two-layer all y^+ wall treatment. To ensure the accurate representation of ship motions, Star-CCM+ offers a Dynamic Fluid-Body Interaction (DFBI) module. This allows the user to select which degrees of freedom the structure analyzed can move and rotate in. For current study, the ship was free to trim and sink.

3.3.3. Mesh generation

The mesh used for calculations was trimmed cells. Meshing and flow simulation were conducted with use of Star-CCM+. The grids generated for DTMB concentrated cell around the hull region of the free surface. In order to avoid using fine grid where it is not necessary local volume were created to sonar dome and assigned particular cell size, To capture the exact flow behavior near the walls of wetted surface prism layers were used to resolve the near-wall flow accurately [10]. Prism layer numbers were selected to ensure that the y^+ value on the ship is maintained at average value 50. To capture the flow around the hull near the free surface, a finer mesh was created in the free surface region. Fig.6 shows the general view of computational mesh for the coarsest mesh.

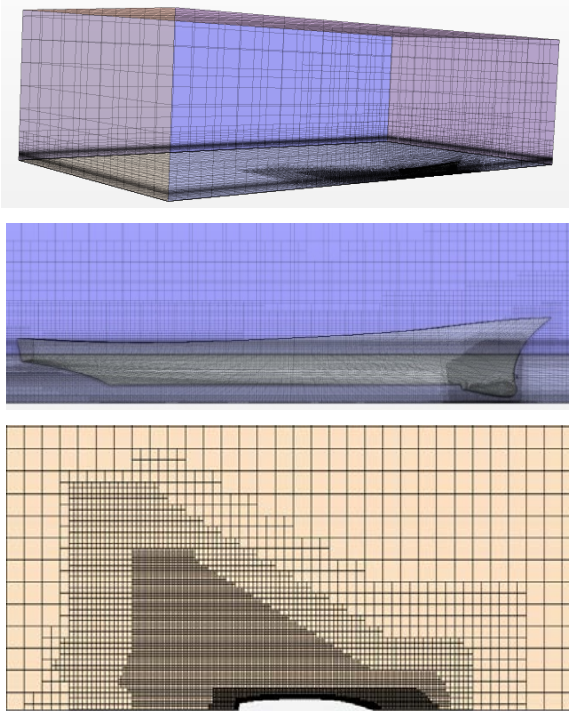


Fig. 6 General view of computational mesh.

3.3.4. Selection of the time step

One of the key issues determining numerical accuracy is time step. For implicit solvers, the time step is decided by the flow features. For standard pseudo-transient resistance computations, the time step is function of the ship length and ship speed [11]

$$\Delta t = 0.005 \sim 0.01L/V \quad (2)$$

Where V is the speed of ship and L is a characteristic length value.

3.4. Result and discussion

3.4.1. Mesh independent study

The first step of research was to carry out the mesh sensitivity study, i.e. to determine the mesh density at which the difference of total resistance obtained from two subsequent meshes reaches sufficiently low value. The goal of such a study is to obtain the "grid-independent solution", i.e. to ensure that further refinement of the mesh does not improve the quality of the result. In presented case, the mesh sensitivity is studied for $Fr_h = 0.703$. Grid studies have been conducted using three grids with Non-integer grid refinement ratio $r_G = \sqrt{2}$ (the value has been recommended by ITTC-Quality Manual 7.5-03-01-01, 2008 [12]) such as coarse (grid#3), medium (grid#2) and fine grid (grid#1)

system corresponding to the cells are 546480, 1208879 and 285565 respectively. Mesh refinement is done by reducing the cell size in all directions outside prism layer. The idea here was to keep the same y^+ values at near-wall cells the all three case equal to around 50.

Table 3 presents the results for total resistance resulting from three grids resolutions at $Fr_h = 0.703$. In presented case showed that, the difference of total resistance obtained from two subsequent meshes (grid#2 and grid #3) reaches sufficiently low value (about 1,0%) so finest mesh was used in further studies. Besides the comparison shows quite good agreement between simulation values (CFD) and experimental values (EXP), especially for the fine mesh (the relative error only 0.65%). The difference between EXP data, D , and CFD simulation, S in this paper defined as:

$$E\%D = \frac{(D-S)}{D} \cdot 100\% \quad (3)$$

Table 3. Predicted total resistance on different grids at $Fr_h = 0.703$.

Parameter		EFD (D)	CFD (F) simulation		
			Grid#3	Grid#2	Grid#1
R_T [N]	Value	30.33	31.87	31.27	31.05
	E%D	-	-5.08	-3.10	-2.37

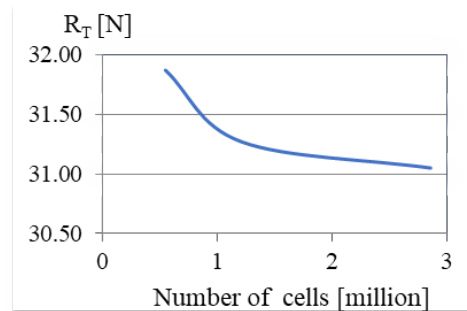


Fig. 7 The relationship between predicted total resistance and mesh density.

3.4.2. Numerical simulation results

Table 4 and Figures 8 shows the comparison of predicted and measured total ship resistance in shallow and deep water with depth Froude number range from 0.302 to 0.755. As can be seen from both table 4 and figure 8, the difference between predicted ship resistance results and experiment results are

from 3 to 7%. The absolute error increase when ship speed increase. Besides, figure 8 shows that the increase in ship resistance in

shallow water compared to deep water at same speed is significantly noticeable, especially near the critical speed region.

Table 4. The predicted ship resistance results in comparison with experimental values

Parameters	Fr _h	0.302	0.502	0.604	0.703	0.755
	V [m/s]	0.598	0.995	1.196	1.394	1.495
R _T [N]	EXP.	3.90	10.87	16.49	30.33	44.50
	CFD	4.15	11.25	16.89	31.05	41.64
Absolute error [N]		-0.25	-0.38	-0.40	-0.72	2.86
Relative error [%]		-6.28	-3.54	-2.45	-2.37	6.43

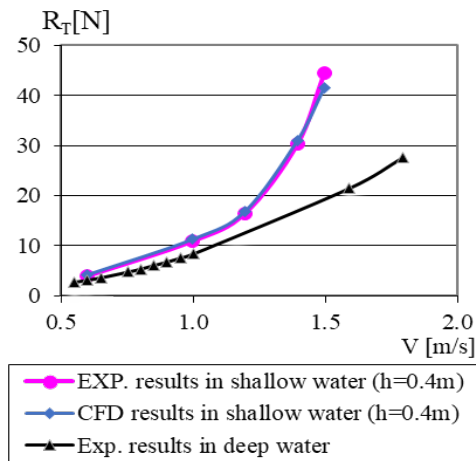


Fig.8. Comparison of deep and shallow water resistance.

The friction, pressure and total resistance coefficients of DTMB model obtained from CFD are showed in table 5 and figure 9 (which is achieved by dividing ship resistance components by $0.5\rho V^2 S$). As can be seen from both table 4 and figure 8, at low speeds, the friction resistance provides the largest contribution to the total resistance, whereas at higher speeds (after Fr_h = 0.703 or V=1.394m/s), the pressure resistance becomes dominant. In addition, the friction resistance decreases rapidly as the velocity scale is moving up. Contrarily, the pressure resistance increases significantly after Fr_h = 0.604 (or V=1.196m/s). Moreover, the friction resistance obtained from CFD is about 1.09 to 1.25 times higher than that obtained by using ITTC 1957, depending on ship speed.

Table 5 The resistance coefficients, obtained from CFD.

Fr _h	V [m/s]	Resistance coefficients from CFD			C _{F*} . 10 ³ (ITTC)
		C _T . 10 ³	C _P . 10 ³	C _V . 10 ³	
0.302	0.598	5.619	1.527	4.092	3.754
0.502	0.995	5.496	1.713	3.783	3.408
0.604	1.196	5.719	1.995	3.723	3.295
0.703	1.394	7.738	4.020	3.718	3.205
0.755	1.495	9.018	5.283	3.735	3.165

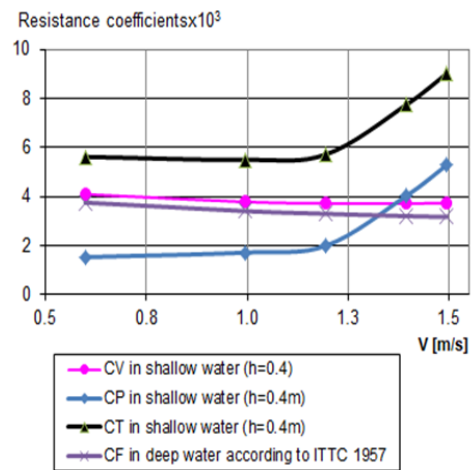


Fig.9 The contributions of the resistance coefficients obtained from CFD

4. Conclusion

Unsteady RANS were performed to predicted resistance of DTMB model in shallow water at different depth Froude numbers. The ship speed values were selected in analogy to the towing tank experiments in CTO [8,9]. All analyses were performed

applying a commercial RANS solver Star-CCM+ version 12.02.011.R8.

The predicted ship resistance and model results were presented for DTMB model. The results show quite good agreement between CFD and experiment for all simulation cases.

The increase in ship resistance in shallow water compared to deep water at same speed is significantly noticeable, especially at near the critical speed region ($Fr_h=0.6\div 1.0$).

The computed results of resistance components (frictional and pressure) illustrate that when ship move in shallow water the pressure resistance component change bigger than friction resistance component, especially at high depth Froude number. It can be explained that wave pattern change due to effect of shallow water. The change of friction resistance can be explained by the increasing the form factor due to the increase of flow velocity under the keel □

5. Acknowledgment

The authors are grateful to the Vietnam Maritime University and CTO for providing necessary research facilities during current research work.

Nomenclature

B [m]:	Ship breadth
L_{PP} [m]:	Length between perpendiculars
L_{WL} [m]:	Length at water level
∇ [m ³]:	Ship volume displacement
S [m ²]	Wetted surface area
T [m]:	Ship draft
R_T [N]	Total ship resistance
C_T [-]	Total ship resistance coefficient
C_F [-]	Frictional ship resistance coefficient
C_P [-]	Pressure resistance coefficient
h [m]	Depth of water
V [m/s]	Ship speed
Fr_h	Depth Froude number
ρ [kg/m ³]	Water density

References

- [1] Artjushkov, L., *Wall effect correction for shallow water model tests*. NE Coast Institution of Engineers and Shipbuilders., 1968.
- [2] Geerts, S., Verwerft, B., Vantorre, M., and Van Rompuy, F., *Improving the efficiency of small inland vessels*. Proc., 7th European Inland Waterway Navigation Conf., Budapest Univ. of Technology and Economics, Budapest, Hungary., 2010.
- [3] Karpov, A., *Calculation of ship resistance in restricted waters*. TRUDY GIL. T. IV, Vol. 2 (in Russian). 1946.
- [4] Linde, F., et al., *Three-Dimensional Numerical Simulation of Ship Resistance in Restricted Waterways: Effect of Ship Sinkage and Channel Restriction*. Journal of Waterway, Port, Coastal, and Ocean Engineering, 2016. 143(1): p. 06016003
- [5] *ITTC 2014 Specialist committee on CFD in marine hydrodynamics—27th ITTC*.
- [6] Larsson, L. and H. Raven, *Ship resistance and flow*. 2010: Society of Naval Architects and Marine Engineers.
- [7] Molland, A.F., S.R. Turnock, and D.A. Hudson, *Ship resistance and propulsion*. 2017: Cambridge university press.
- [8] *Resistance test report in deep water for DTMB vessel*. CTO, Poland 2017.
- [9] *Resistance test report in shallow water for DTMB vessel*. CTO, Poland 2017.
- [10] *CD-Adapco. UserguideSTAR-CCM ρ Version 12.0.2,2017*.
- [11] *ITTC 2011b Recommended procedures and guidelines 7.5-03-02-03*.
- [12] *ITTC-Quality Manual 7.5-03-01-01, 2008*.

Ngày nhận bài: 8/3/2018

Ngày chuyển phản biện: 12/3/2018

Ngày hoàn thành sửa bài: 3/4/2018

Ngày chấp nhận đăng: 9/4/2018